


# Sexual Dimorphism in the Extracellular and Pericellular Matrix of Articular Cartilage

CARTILAGE  
 July-September 2022: 1–15  
 © The Author(s) 2022  
 DOI: 10.1177/19476035221121792  
[journals.sagepub.com/home/CAR](https://journals.sagepub.com/home/CAR)  


Paula A. Hernandez<sup>1</sup> , Miranda Moreno<sup>1</sup> , Zahra Barati<sup>1</sup>, Conner Hutcherson<sup>1</sup>,  
 Adwait A. Sathe<sup>2</sup>, Chao Xing<sup>2,3,4</sup> , Jamie Wright<sup>5</sup>, Tre Welch<sup>5</sup> ,  
 and Yasin Dhafer<sup>1,6</sup>

## Abstract

**Objective.** Women have a higher prevalence and burden of joint injuries and pathologies involving articular cartilage than men. Although knee injuries affecting young women are on the rise, most studies related to sexual dimorphism target postmenopausal women. We hypothesize that sexual dimorphism in cartilage structure and mechanics is present before menopause, which can contribute to sex disparities in cartilage pathologies. **Design.** Bovine knee was used as a model to study healthy adult cartilage. We compared elastic moduli under compression, abundances of extracellular and pericellular matrix (PCM) proteins using proteomics, and PCM constituency with tissue immunofluorescence. The gene expression of matrix-related genes under basal, anabolic, and catabolic conditions was assessed by quantitative polymerase chain reaction (qPCR). **Results.** The equilibrium modulus was higher in male cartilage compared with female cartilage. Proteoglycans were not associated with this biomechanical dimorphism. Proteomic and pathway analyses of tissue showed dimorphic enriched pathways in extracellular matrix (ECM)-related proteins in which male cartilage was enriched in matrix interconnectors and crosslinkers that strengthen the ECM network. Moreover, male and female tissue differed in enriched PCM components. Females had more abundance of collagen type VI and decorin, suggesting different PCM mechanics. Furthermore, the activation of regenerative and catabolic function in chondrocytes triggered sex-dependent signatures in gene expression, indicating dimorphic genetic regulation that is dependent on stimulation. **Conclusions.** We provide evidence for sexual dimorphism in cartilage before menopause. Some differences are intrinsic to chondrocytes' gene expression defined by their XX versus XY chromosomal constituency.

## Keywords

sex differences, articular cartilage, extracellular matrix, pericellular matrix

## Introduction

In most biological and clinical studies, sexual dimorphism has been addressed—for the most part—as an equivalent inclusion of males and females with *post hoc* analyses on the aggregate response. Although informative, these examinations miss the opportunity to explore the pivotal role that chromosomal sex may play in fundamental biological processes. The significance of addressing sex differences in the musculoskeletal system is shown by the following: Women have a higher susceptibility than men to joint injuries, such as those affecting the anterior cruciate ligament (ACL) in the knee<sup>1,2</sup>; women have a higher risk of developing osteoarthritis (OA) that is posttraumatic (posttraumatic osteoarthritis [PTOA]) after ACL injury<sup>3</sup>; and women are more severely affected by knee OA than men.<sup>4,5</sup> Cartilage degeneration is the hallmark of OA. Understanding and embracing sex differences in cartilage biology, mechanics, and

<sup>1</sup>Department of Orthopedic Surgery, University of Texas Southwestern Medical Center, Dallas, TX, USA

<sup>2</sup>Eugene McDermott Center for Human Growth and Development, University of Texas Southwestern Medical Center, Dallas, TX, USA

<sup>3</sup>Department of Bioinformatics, University of Texas Southwestern Medical Center, Dallas, TX, USA

<sup>4</sup>Department of Population and Data Sciences, University of Texas Southwestern Medical Center, Dallas, TX, USA

<sup>5</sup>Department of Cardiovascular and Thoracic Surgery, University of Texas Southwestern Medical Center, Dallas, TX, USA

<sup>6</sup>Department of Physical Medicine & Rehabilitation, University of Texas Southwestern Medical Center, Dallas, TX, USA

Supplementary material for this article is available on the *Cartilage* website at <http://cart.sagepub.com/supplemental>.

### Corresponding Author:

Paula A. Hernandez, Department of Orthopaedic Surgery, University of Texas Southwestern Medical Center, 5323 Harry Hines Blvd, Dallas, TX 75390, USA.

Email: [Paula.Hernandez2@UTsouthwestern.edu](mailto:Paula.Hernandez2@UTsouthwestern.edu)



repair may generate opportunities to develop tailored interventions.

To date, most explorations of sexual dimorphism have been contextualized in the chondrogenic potential of stem cells<sup>6,7</sup> and the response of mature chondrocytes to sex-specific hormones.<sup>8-10</sup> Identifying sex-intrinsic differences in the ability of chondrocytes to synthesize and maintain their extracellular matrix (ECM) has significant scientific and clinical implications. For example, better clinical results have been observed in men than women after autologous chondrocyte implantation (ACI),<sup>11</sup> but the underlying mechanism for this is still unknown. These facts led us to investigate whether ECM composition and mechanics are sexually dimorphic.

Here, we hypothesize that sexual dimorphism in cartilage is present before menopause, which can contribute to the sexual disparities in cartilage affecting diseases. Due to the limitations of obtaining healthy and young adult human cartilage, we have used bovine knee as a model. We tested mechanical properties, abundance of ECM and pericellular matrix (PCM) proteins, and gene expression under basal, anabolic, and catabolic conditions. Altogether, we provide insights into the hallmarks of sexual dimorphism and a motivation to fully decode the mechanical, molecular, and regulatory mechanisms that lay behind them.

## Method

### *Cell Culture and Treatments*

Six stifle joints from adult cattle, between 24 and 30 months old, were obtained from a local abattoir (6♀, 6♂). The sex of the samples was corroborated with a polymerase chain reaction (PCR) targeting *Bos taurus* gene for DEAD box protein (DDX3X and DDX3Y),<sup>12</sup> as shown in Supplementary methods and Supplementary Figure S1. Articular cartilage was dissected from the femoral condyle. Tissue was digested with 0.2% pronase (Roche) in complete media (Dulbecco's Modified Eagle Medium [DMEM] high glucose + 10% heat-inactivated fetal bovine serum + 1x antibiotics-antimycotics + 50 µg/ml ascorbic acid) for 1 hour at 37°C, followed by 0.2% collagenase D (Roche) in complete media for 17 hours at 37°C in gentle agitation. Digested cells were passed through a 100-µm cell strainer and washed in phosphate-buffered saline (PBS). Cells were expanded in complete media for less than 10 days and used as passage 0, or expanded further, up to passage 2. For IL-1β treatment, cells in passage 0 were incubated in serum-free media with or without 10 ng/ml bovine recombinant IL-1β for 24 hours.

### *RNA Extraction and quantitative PCR (qPCR)*

Total RNA was extracted from cells using RNeasy columns (QIAGEN) following the manufacturer's instructions.

Briefly, 1 µg of total RNA was used to convert to cDNA with an iScript conversion kit (Bio-Rad). From that, 12.5 ng were used for each qPCR reaction by employing iTaq Universal SYBR green supermix (Bio-Rad) in a CFX96 qPCR machine (Bio-Rad). The relative quantity to normalizer was calculated using  $2^{-\Delta C_t}$  with the geometric mean of GAPDH and 18S for basal and catabolic conditions. For regenerative function, we used 18S and SDHA as normalizers. Bovine primers are summarized in Supplementary Table S1. Primers for bovine decorin (DCN) and HSPG2 were obtained from Bio-Rad.

### *Immunohistochemistry*

Fresh cartilage samples were snap-frozen in liquid nitrogen and embedded in optimal cutting temperature (OCT) for cryosectioning. Slides of 5 µm thickness were kept cold and fixed in 10% neutralized buffered formalin for 10 minutes at room temperature. Slides were washed twice for 5 minutes each with PBS, blocked for 1 hour at room temperature in 5% bovine serum albumin (BSA) with 10% goat serum in PBS, and incubated with primary antibodies in tris-buffered saline (TBS) + 0.1% Tween 20 (TBST) containing 2% BSA overnight at 4°C. Primary antibodies used were anti-collagen VI (Novus Biologicals, NB120-6588, 1:300), anti-perlecan (Novus Biologicals, NBP-0570, 1:100), anti-collagen IX (Novus Biologicals, NBP2-92796, 1:120), and anti-decorin (Abcam, ab181456, 1:100). Negative controls were done by omitting the primary antibody. After washing 3 times for 10 minutes each in TBS + 0.2% Tween 20 at room temperature with gentle shaking, slides were incubated with secondary antibody goat anti-rabbit Alexa 488 or anti-mouse Alexa 594 (Molecular Probes, 1:1000) for 1 hour at room temperature in 5% BSA-TBST in the dark. Slides were washed 3 times for 10 minutes each in TBS + 0.2% Tween 20 at room temperature with gentle shaking in the dark. Slides were stained for 3 minutes at room temperature with 4',6-diamidino-2-phenylindole (DAPI; Invitrogen, D1306) for nuclear counterstain. After 2 quick washes with PBS and 1 rinse with MilliQ water, slides were mounted using Vectashield (Vector Laboratories). Pictures were taken using a Zeiss LSM880 Airyscan confocal microscope. The same exposure conditions were used for all samples with the same antigen and their corresponding negative controls. Images were processed in ImageJ (U.S. National Institutes of Health, Bethesda, Maryland, USA; <https://imagej.nih.gov/ij/>).

### *Proteoglycan Staining and Quantification*

Cartilage slides of 5 µm thickness were obtained from paraffin-embedded blocks. Slides were de-paraffinized and rehydrated for safranin-O staining. Slides were subjected to the following steps: Weigert's iron hematoxylin for 5

minutes, 4 washes with distilled water, 1% acid alcohol for 2 seconds, and washed 3 times with distilled water. For better quantification, we omitted the use of fast green as previously described.<sup>13</sup> We added 1% acetic acid for 45 seconds, 1% safranin-O stain for 30 minutes, washed with ethanol (95%) 3 times, and washed with xylene 2 times. Slides were mounted using Permount (Fisher). For quantification of glycosaminoglycans (GAG) content, images were converted to 8-bit and gray intensity after calibration was measured using ImageJ. Optical density for 6 animals per sex was analyzed using GraphPad v9.1.

### **Cells and Proteoglycan Depletion of Cartilage Samples (Collagen-Enriched Samples)**

Full-thickness cartilage without subchondral bone was obtained from bovine femoral condyle using sharp dissection. Samples were collected using 6 mm diameter punches and immediately frozen in PBS-soaked gauze at  $-80^{\circ}\text{C}$  until further use. To remove proteoglycans, cells, and nuclear material, we used a previously described protocol<sup>14</sup> with some modifications. After 24 hours of chondroitinase digestion, samples were incubated with 1% sodium dodecyl sulfate (SDS) in hypotonic buffer with protease inhibitor cocktail for 24 hours at room temperature. After that, samples were washed for 24 hours with PBS at room temperature and constant agitation. Removal of nuclear material was confirmed by staining a thin layer of cartilage with DAPI and visualizing it in a fluorescence microscope (Nikon Eclipse Ti).

### **Mechanical Analysis**

We used 1 to 2 full-thickness cartilage samples without subchondral bone per animal (6♀ and 6♂). We measured sample thickness and corroborated diameter of 6 mm using a digital caliper (Cen-Tech) and then loaded them (subchondral bone interface down) onto a Bose Electroforce 3200 Analyzer (TA Instruments; New Castle, DE). We used a 2.45 N or 450 N load cell, depending on the stiffness of the sample, in unconfined compression between two stainless steel compression plates. The sample was placed within a sandpaper-lined 150 mm tissue culture dish (Corning; Corning, NY) and submerged in PBS. The sample was secured between the compression plates with an initial small normal load of 0.1 N to generate uniform contact between the plates, to keep the sample flat, and to maintain positioning during PBS filling. After immersion at room temperature, samples were allowed to sit and equilibrate for at least 1 hour or until the gap between plates remained constant. The gap at this point was noted to ensure proper strain calculations. The prestress resulting from the 0.1 N preload was not significantly different between males and females (Suppl. Fig. S2). After the plate gap reached a steady state,

samples underwent stepwise stress relaxation to compressive strains of 2%, 4%, 6%, 8%, and 10% at a rate of 0.050 mm/s. TA Wintest software (TA Instruments; New Castle, DE) was used to collect data at 100 points/second sampling rates. Samples were compressed stepwise then held constant for 45 minutes. The final Cauchy stress value at each step (averaged over the final 200 s of readings) was recorded and calculated as the equilibrium stress at the given strain using MATLAB software (MathWorks Inc.; Natick, MA). Equilibrium stress was then collected at each of the five strain levels and plotted versus incremental strain. Modulus calculations were made from the linear portion of the equilibrium curves.

### **Proteomics**

Decellularized samples from 6 animals per sex were snap-frozen in liquid nitrogen and pulverized using a mortar and pestle. The powder was suspended in 5% SDS with 50 mM of triethylammonium bicarbonate (TEAB) in a ratio of 500  $\mu\text{l}$  per 100 mg of powder. Dithiothreitol (DTT) was added to a final concentration of 10 mM, and samples were incubated at  $57^{\circ}\text{C}$  for 30 minutes. After cooling, iodoacetamide was added to a final concentration of 20 mM, and samples were incubated for 30 minutes at room temperature in the dark. Following centrifugation for 2 minutes at 13,200 rpm, the supernatants were removed, of which 50  $\mu\text{l}$  of each sample were digested overnight with trypsin at  $37^{\circ}\text{C}$  using an S-Trap (ProtiFi). Following digestion, the peptide eluate was dried and reconstituted in 100 mM of TEAB buffer. The remaining pellets were washed with 100 mM of TEAB (pH 8.0) 3 times. Then, 50  $\mu\text{l}$  of 8 M urea in 100 mM of TEAB (pH 8.0) buffer was added to suspend each pellet, and these were diluted with 10 mM of  $\text{CaCl}_2$  and 100 mM of TEAB (pH 8.0) to bring the final urea concentration below 2 M. This solution was digested at  $37^{\circ}\text{C}$  with Lys-C for 2 hours, followed by overnight trypsin digestion. After digestion, the slurry was centrifuged, and the supernatant was removed and cleaned using an MCX uElution SPE plate (Waters). The peptides were dried and reconstituted in 100 mM of TEAB and combined with their initial corresponding supernatant digests. The samples were labeled with Tandem Mass Tag (TMT) reagent, quenched with 5% hydroxylamine, and combined. These were dried using an HLB uElution plate (Waters), reconstituted in a 2% acetonitrile, 0.1% trifluoroacetic acid (TFA) buffer, and injected onto an Orbitrap Fusion Lumos mass spectrometer coupled to an Ultimate 3000 RSLC-Nano liquid chromatography system. Samples were injected onto a 75  $\mu\text{m}$  i.d., 75-cm long EasySpray column (Thermo Scientific) and eluted with a gradient from 0% to 28% buffer B over 180 minutes. Buffer A contained 2% (v/v) acetonitrile (ACN) and 0.1% formic acid in water, and buffer B contained 80% (v/v) ACN, 10% (v/v) trifluoroethanol, and 0.1% formic acid in

water. The mass spectrometer operated in positive ion mode with a source voltage of ~2 kV and an ion transfer tube temperature of 275°C. MS scans were acquired at 120,000 resolution in the Orbitrap, and top speed mode was used for SPS-MS3 analysis with a cycle time of 2.5 seconds. MS2 was performed with collision induced dissociation (CID) with a collision energy of 35%. The Top 10 fragments were selected for MS3 fragmentation using higher-energy C-trap dissociation (HCD) with a collision energy of 58%. Dynamic exclusion was set for 25 seconds after an ion was selected for fragmentation. Raw MS data files were analyzed using Proteome Discoverer v2.4 SP1 (Thermo Scientific), with peptide identification performed using Sequest HT searching against the bovine protein database from UniProt. Fragment and precursor tolerances of 10 ppm and 0.6 Da were specified, and three missed cleavages were allowed. Carbamidomethylation of Cys and TMT labeling of N-termini and Lys side chains were set as a fixed modification, with oxidation of Met being set as a variable modification. The false discovery rate cutoff was 1% for all peptides. Results are shown in Supplementary Table S2.

### *Transforming Growth Factor- $\beta$ 3 (TGF- $\beta$ 3) Treatment in Alginate Beads*

After trypsinization,  $2 \times 10^6$  cells were suspended in 1 ml of 1.2% alginate solution. Beads were prepared as previously described<sup>15</sup> and grown in chondrogenic media (DMEM high glucose, 1% insulin-transferin-selenium [Sigma-Aldrich]), 1% nonessential amino acids (Gibco), 1% antibiotic-antimycotic solution (Gibco), and 50  $\mu$ g/ml of ascorbic acid containing 10 ng/ml of TGF- $\beta$ 3 (R&D Systems, 8420). Media was replaced twice a week.

### *Statistical Analysis*

Statistical analysis was performed in GraphPad v9.1. For mechanic data, linear regression models were fitted and slopes of regression were compared using analyses of covariance (ANCOVAs). Sample thicknesses were averaged and compared using a two-tailed unpaired Student's *t* test. For proteoglycan content, we used two-way analyses of variance (ANOVAs) followed by Sidak's multiple comparison test. To compare mRNA expression of female chondrocytes versus male chondrocytes, we used a two-tailed unpaired Student's *t* test. To compare sex differences in response to TGF- $\beta$ 3, we used repeated measures two-way ANOVAs followed by Sidak's multiple comparisons test. To evaluate changes in gene expression in response to TGF- $\beta$ 3 with time, we used a repeated measures two-way ANOVA followed by Dunnett's multiple comparisons test. To evaluate the effect of sex on the relative quantities of mRNA with IL-1 $\beta$ , we used a two-tailed unpaired Student's *t* test. In all analyses,  $P < 0.05$  was considered statistically significant.

To account for differences in protein abundance in the samples and the batch effects (2 batches), we utilized the function TAMPOR, implemented by Johnson and colleagues.<sup>16</sup> It is based on Tukey's median polish correcting for both abundance differences in samples and batch effects. Both sample-wise and protein-wise median centering is performed. We log<sub>2</sub>-transformed the resulting abundance data following normalization. We implemented the Unpaired Student's *t* test assuming unequal variance to calculate significance levels as *P* values and adjust using the method Benjamini and Hochberg (BH) for False Discovery Rate (FDR) calculation.<sup>17</sup> FDR values were higher than expected primarily due to variability between samples (non-environmentally controlled farm animals) and to the limited number of proteins obtained from collagen-enriched samples. Therefore, for significance ( $P < 0.05$ ) in proteomics results, we considered *P* value instead of the adjusted *P* value.

## **Results**

### *Dimorphism in Cartilage Network Mechanics*

The equilibrium modulus of articular cartilage depends on the intactness of both collagen and proteoglycan networks.<sup>18,19</sup> In this study, we used a stress relaxation test in bovine cartilage to determine the equilibrium compressive modulus in unconfined compression (**Fig. 1A**). We observed an average modulus of 251.3 kPa for male cartilage and 73.4 kPa for female cartilage (**Fig. 1B**)—a 3.4-fold higher difference for males. Explant thickness was not significantly different between males and females (**Fig. 1C**). The average weight of the animals was 489 kg  $\pm$  50 kg for males and 382 kg  $\pm$  90 kg for females ( $\pm$ SD;  $P = 0.07$ ; two-tailed unpaired Student's *t* test).

We next evaluated the individual contribution of the collagen network and proteoglycans to the observed dimorphism. For proteoglycans, first we used viscoelastic modeling to calculate the relaxation time at 8% strain. A lower relaxation time indicates a higher permeability and a faster loss of liquid under compression. We found no differences in relaxation time between males and females (Suppl. Fig. S3). Next, we investigated the proteoglycan content of male and female cartilage samples using histological analysis. For this, we employed a previously described method using safranin-O staining with no fast green.<sup>13</sup> A stronger safranin-O staining was found only in the deep zone of male cartilage compared with female (**Fig. 2A, B**). We hypothesize that if proteoglycans are responsible for the observed mechanical dimorphism, then removing them would eliminate the differences between sexes. To evaluate this, we decellularized the samples and partially depleted proteoglycans using a previously described protocol,<sup>14</sup> resulting in what we call "collagen-enriched samples." Although the reduction of proteoglycan content affects

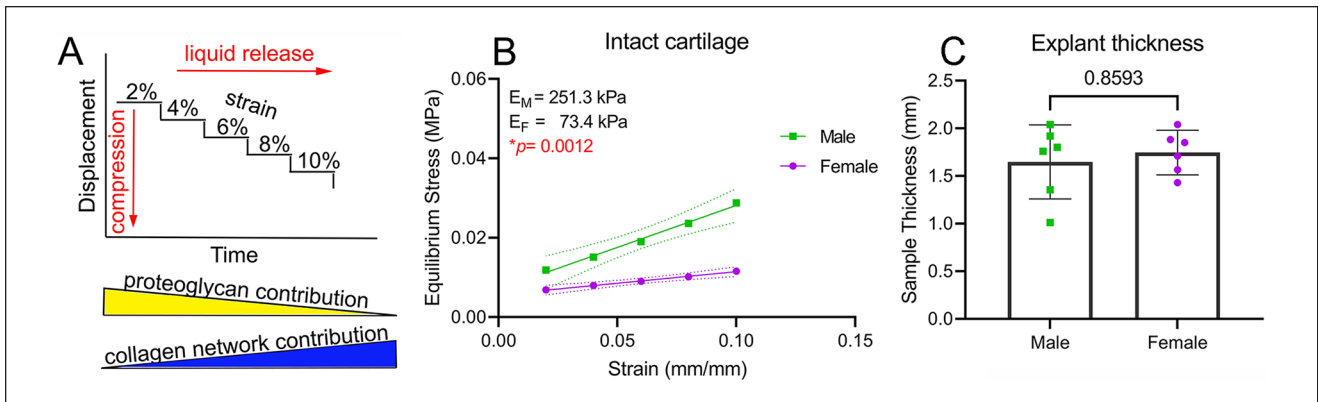


**Figure 1.** Dimorphism in cartilage network mechanics. **(A)** Schematics of the stress relaxation test used. The expected relative contribution of proteoglycans and collagen networks to equilibrium modulus are indicated at the bottom of the graph. **(B)** Equilibrium modulus calculated from the linear portion of the stress-strain curve in intact cartilage. **(C)** Sample thickness of intact cartilage samples. Data in B and C are presented as mean  $\pm$  95% CI (dotted lines in B);  $n = 6\sigma$  and  $6\varphi$ , with each measured in duplicate. CI = confidence interval.

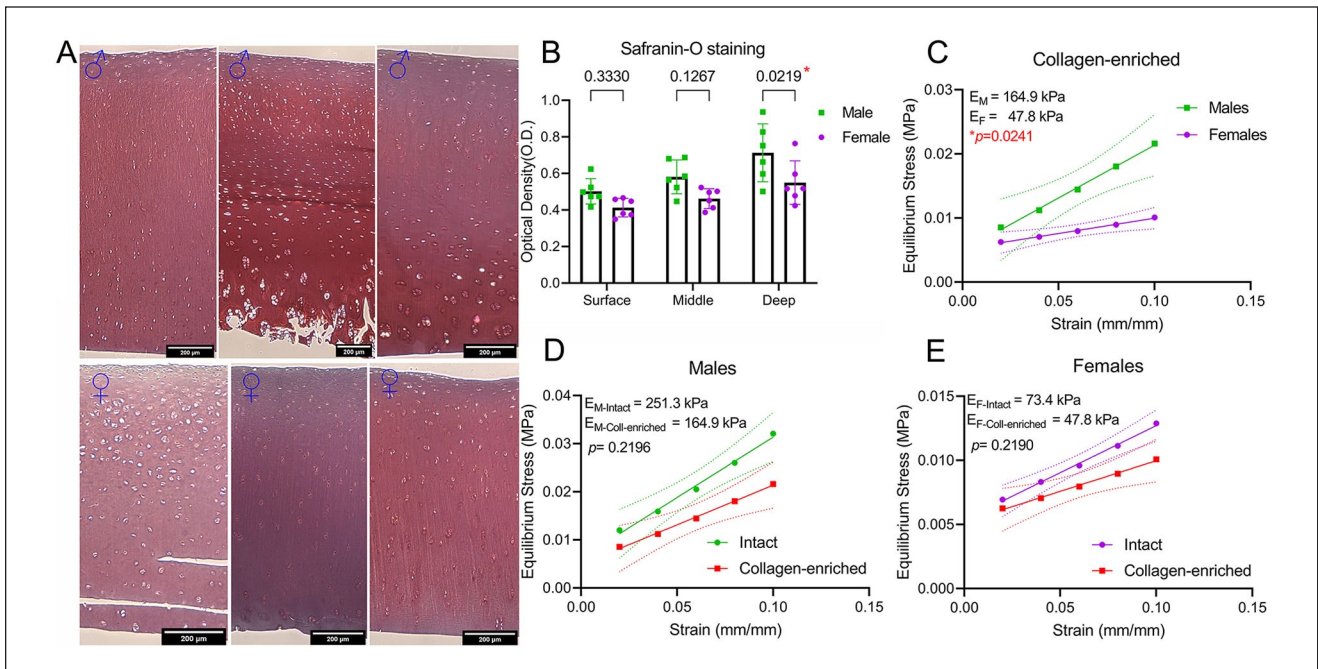


**Figure 2.** Proteoglycans are not responsible for mechanical dimorphism. **(A)** Representative images of safranin-O staining of male and female cartilage. Fast green was omitted. Scale bars are 200  $\mu$ m. **(B)** Quantification of optical density from safranin-O staining in surface, middle, and deep layers;  $n = 6\sigma$  and  $6\varphi$ , mean  $\pm$  SD. **(C)** Stress-strain curve showing calculated equilibrium moduli for male and female tissue. Proteoglycans were digested with chondroitinase ABC. **(D-E)** Stress-strain slopes and equilibrium modulus of males and females comparing intact with proteoglycan-depleted cartilage. Data in C-E are presented as mean  $\pm$  95% CI (dotted lines in C-E);  $n = 6\sigma$  and  $6\varphi$ , with each measured in duplicate.

cartilage mechanics, it has been shown that this protocol does not disrupt collagen matrix.<sup>20</sup> To avoid potential artifacts due to non-equivalent proteoglycan depletion, we performed this protocol simultaneously in both female and male samples. Subsequently, these collagen-enriched samples were subjected to the same stepwise stress relaxation

protocol used for intact samples. Results revealed an average equilibrium modulus of 164.9 kPa for male samples and 47.8 kPa for female samples. Similar to intact cartilage, males had a 3.45-fold higher modulus compared with females (**Fig. 2C**). In fact, proteoglycan depletion equally reduced the moduli of male and female cartilage by

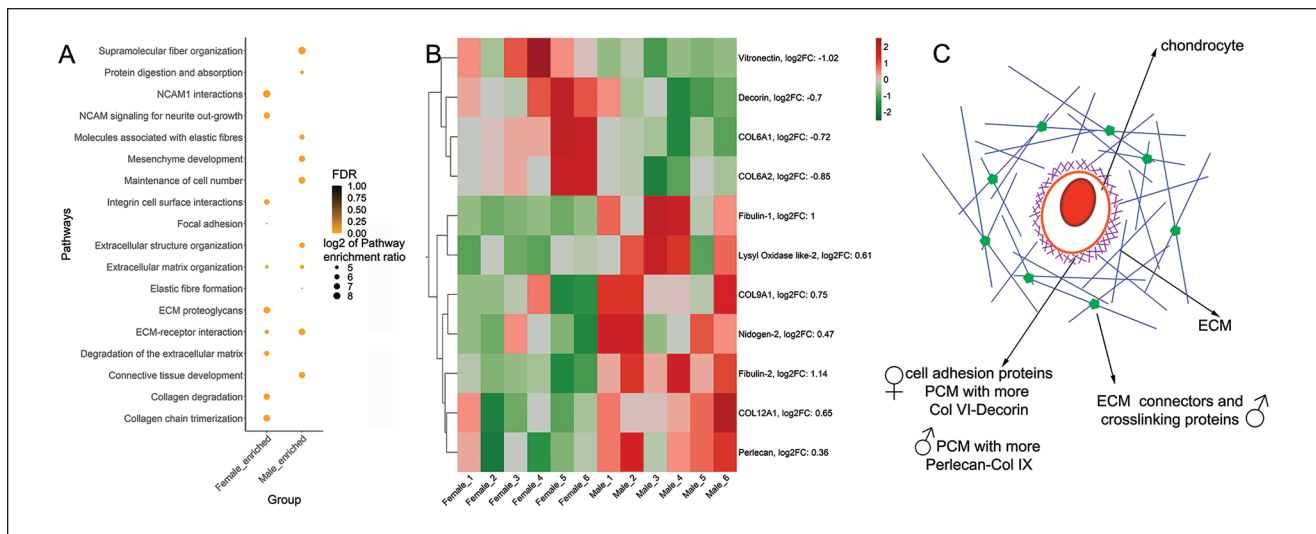


**Figure 3.** Dimorphic enrichment of ECM proteins in male and female cartilage. **(A)** Pathway analysis of protein abundances in male and female cartilage. **(B)** Heat map with ECM proteins showing a significant difference in male and female cartilage. Upregulation is shown in red and downregulation is shown in green. Fold change of male compared with female is indicated in parenthesis;  $n = 6\sigma + 6\varphi$ . **(C)** Summary schematics of main protein functions enriched in female and male cartilage. Male cartilage was enriched in ECM connectors and crosslink proteins, whereas female cartilage was enriched in PCM proteins and cell matrix adhesion regulators. A-B: Empirical Bayes moderated  $t$  test implemented in limma. ECM = extracellular matrix; FDR = False Discovery Rate; PCM = pericellular matrix; NCAMI = neural cell adhesion molecule 1.

1.5-fold compared with the corresponding intact cartilage (**Fig. 2D, E**).

### Differential Enrichment of ECM Proteins in Male and Female Cartilage

Because cells and proteoglycan do not appear to be responsible for the observed sex-dependent mechanical differences, we hypothesized that collagen network-related components are the drivers of the observed higher stiffness in male cartilage. To investigate dimorphism in collagen components, we performed a proteomic analysis of the collagen-enriched fraction of the samples. Proteomic analysis, including proline and methionine oxidation as variable modifications, identified 224 proteins (Suppl. Table S2). Because cells and proteoglycan depletion also removed nonstructural proteins, we did not detect associated metalloproteases (MMPs) or a disintegrin and metalloproteinase with thrombospondin motifs (ADAMTSs), but other matrix proteases such as HtrA1 (which showed no sex differences) were detected. In addition, a small number of cellular proteins that could result from incomplete removal of the cellular fraction were also present.

Pathway analysis using WebGestalt (WEB-based Gene Set Analysis Toolkit)<sup>21</sup> confirmed differences between males and females (**Fig. 3A**). The reference data sets used were as follows: (1) pathway gene sets from biological processes of the Gene Ontology resource (<http://www.geneontology.org/>), (2) molecular pathways of the Reactome

database (<http://www.reactome.org/>), and (3) molecular pathways of the KEGG database (<https://www.genome.jp/kegg/>). Pathways enriched in male tissue were related to supramolecular fiber organization, molecules associated with elastic fibers, extracellular structure organization, ECM-receptor interaction, and connective tissue development. In female tissue, among the enriched pathways, we found integrin cell surface interactions, ECM proteoglycans, degradation of the ECM, collagen degradation, and collagen chain trimerization. The higher elastic modulus found in male tissue could be related to an increased enrichment in pathways associated with the ECM structure organization. To evaluate this possibility, we explored the abundance of proteins present in male and female collagen-enriched cartilage samples. Surprisingly, no dimorphism in collagen type II was found (**Fig. 3B**). Instead, only 11 ECM members—collagenous and noncollagenous proteins—were found to have contrasting abundances in males compared with females (**Fig. 3B**). However, these proteins have relevant functions in matrix assembly, crosslinking, and mechanics, in agreement with the pathway analysis. Overall, male tissue was enriched in ECM connectors and cross-linkers such as LOXL-2 and fibulins-1 and -4, whereas female tissue was enriched in the cell matrix connector vitronectin. Moreover, male and female tissues differed in the enrichment of their PCM components. There was a higher abundance of collagen type VI alpha 1 and alpha 2 and decorin in females, and a higher abundance of perlecan and collagen type IX alpha 1 in males (**Fig. 3B**).

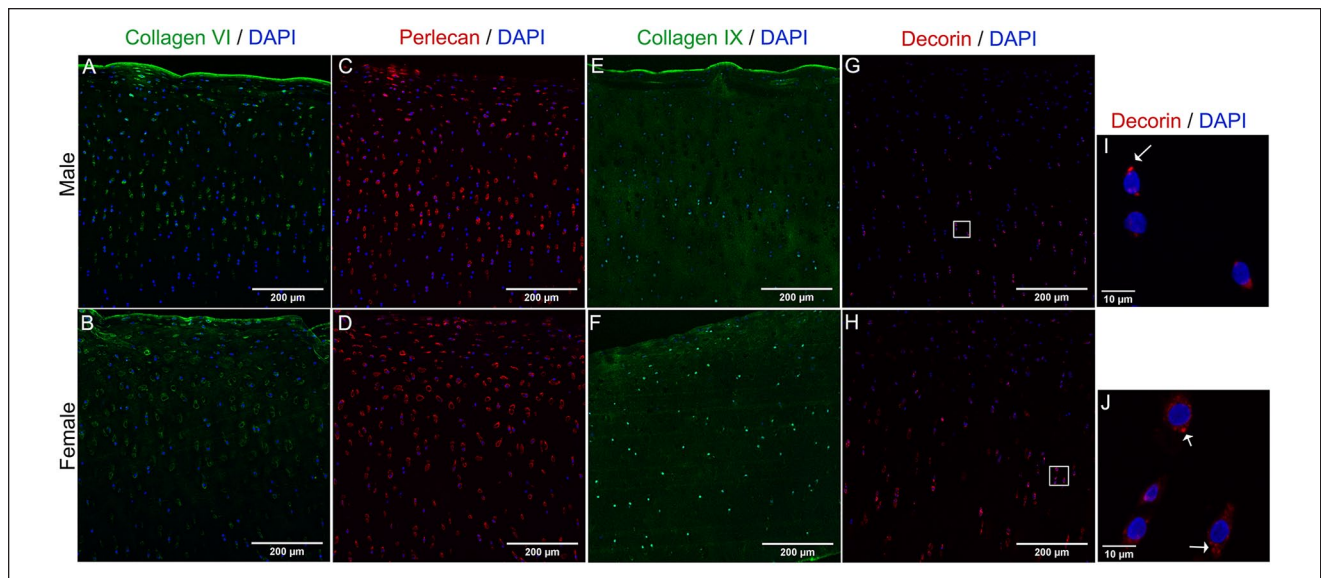


**Figure 4.** Dimorphic abundance of PCM proteins in male and female cartilage. Representative images of Z-project with maximum intensity of collagen type VI (**A, B**), perlecan (**C, D**), collagen type IX (**E, F**), and decorin (**G, H**) in cartilage sections. DAPI was used for nuclear counterstain (blue). Scale bars are 200  $\mu\text{m}$ . A higher magnification of chondrocytes stained for decorin (**I, J**) reveals an accumulation of this protein inside the cell, as indicated by white arrows. Scale bars are 10  $\mu\text{m}$ . Brightness was adjusted equally in males and females for display purposes only. DAPI = 4',6-diamidino-2-phenylindole; PCM = pericellular matrix.

In summary, we found that male cartilage has an enrichment in proteins and pathways associated with stabilizing the ECM structure, while female cartilage is enriched in cell-ECM connectors. There is dimorphism in the PCM composition, which could have significant consequences on mechanotransduction (**Fig. 3C**).

### Differential PCM Protein Abundance

To validate our proteomics results regarding PCM composition, we performed tissue immunofluorescence staining of collagens type VI, IX, decorin, and perlecan. Collagen type VI was detected at the surface layer and in the vicinity of chondrocytes throughout cartilage layers. The most evident difference was that in female cartilage, collagen VI was found also in the interterritorial areas of the ECM in the middle area (**Fig. 4A, B**). Perlecan was present similarly in male and female tissue, and it was mostly restricted to the PCM area. Perlecan was distributed throughout all layers of cartilage (**Fig. 4C, D**). Collagen type IX was found distributed in most of the tissue. In males, the staining was strong in the surface and interterritorial areas of the middle layer. In females, collagen IX staining was stronger at the tissue surface, and in what appears to be intracellular staining as well (**Fig. 4E, F**). Decorin staining was stronger toward the deep areas of cartilage in both males and females, with the staining more intense in female tissue (**Fig. 4G, H**). The staining pattern in the PCM was not as clear as for perlecan. A higher magnification of images of decorin staining

showed an accumulation of this protein inside the cells in both male and female chondrocytes (**Fig. 4I, J**). In summary, we found sex differences in the intensity and pattern of staining for collagens type VI and IX, and decorin.

### Dimorphism in Unstimulated Chondrocyte Monolayers or “Basal” Conditions

Among possible mechanisms for the observed dimorphism in ECM and PCM proteins is that male and female chondrocytes express these targets differentially depending on their chromosomal sex (XX vs. XY) and/or that the tissue remodeling is dimorphic. To test the first option, we explored sex differences in the mRNA expression of a group of ECM components (COL2A1, ACAN, COL10A1, and COL11A1), the master chondrogenic transcription factor SOX9, PCM components (COL6A1, COL9A1, DCN, and HSPG2), the basal expression of MMPs (MMP-1, MMP-3, MMP-9, MMP-13, and ADAMTS-4, ADAMTS-5), and their inhibitors (tissue inhibitor of metalloproteases [TIMP]-1, TIMP-2) using chondrocyte monolayers at an early stage of cell expansion, that is, in passage 0. Because chondrocytes were not exposed to additional external stimulation such as mechanical load or chondrogenic factors, we call these “basal” conditions. Although the expression of COL2A1 and ACAN was similar in male and female cells (**Fig. 5A, B**), the expression of SOX9 was higher in male chondrocytes (**Fig. 5C**). We did not detect differences in COL10A1 and COL11A1. Nevertheless, in agreement with our proteomics data,

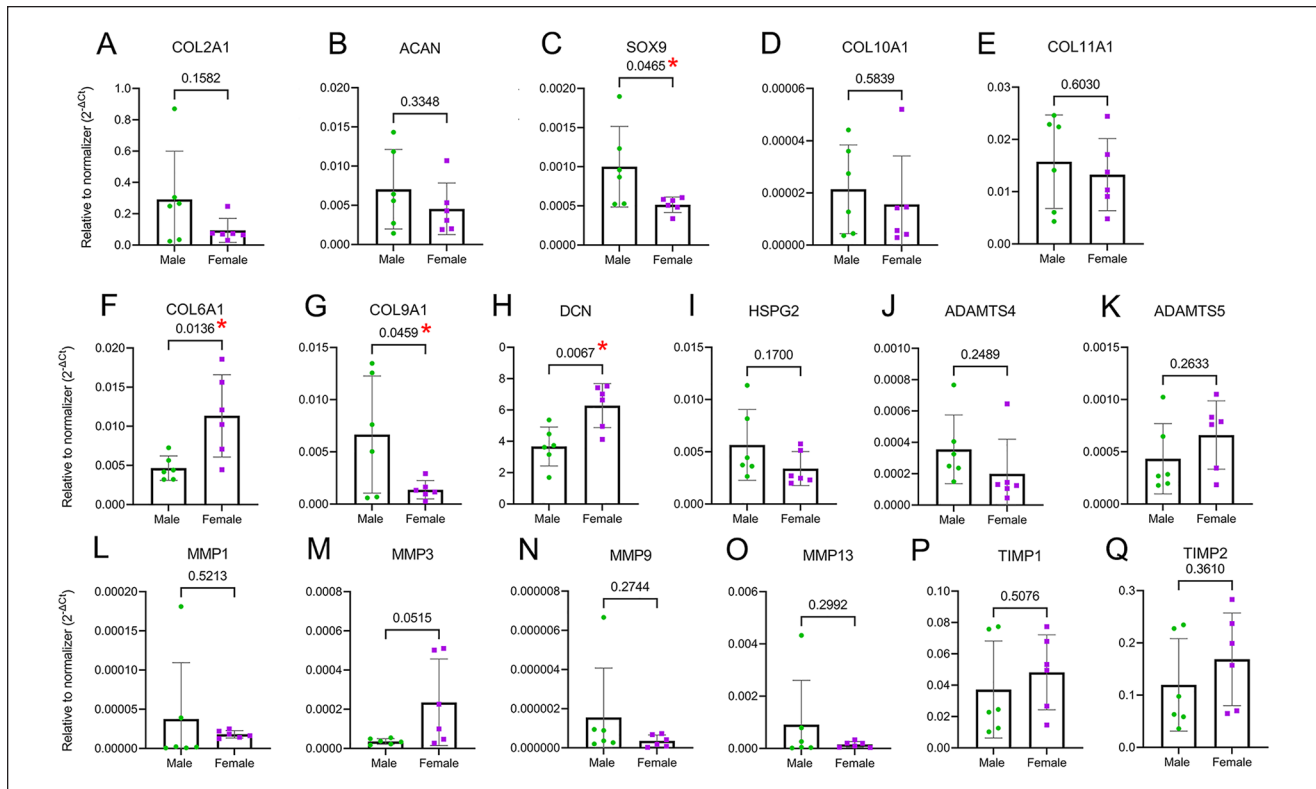


**Figure 5.** Chondrocytes show sexual dimorphism in gene expression of PCM proteins. **(A-B)** No difference between male and female was detected in the expression of COL2A1 and ACAN. **(C)** SOX9 was higher in male chondrocytes. **(D-E)** COL10A1 and COL11A1 were not dimorphic. **(F-H)** The PCM genes COL6A1, COL9A1, and DCN were expressed in a sex-dependent manner, although HSPG2 **(I)** was not dimorphic. **(J-K)** No difference was observed in ADAMTS4 and ADAMTS5 expression. **(L-O)** MMP1, MMP9, and MMP13 were similar between sexes, but MMP3 showed a trend for higher expression in females. **(P-Q)** None of the TIMPs tested were differentially expressed depending on the sex of the cell. Data are presented as mean  $\pm$  SD of relative quantity to normalizer (geometric mean of 18S and GAPDH). Cells from 6 $\sigma$  + 6 $\phi$  were used in passage 0. PCM = pericellular matrix; MMP = metalloprotease; ADAMTS = a disintegrin and metalloproteinase with thrombospondin motifs; DCN = decorin; TIMP = tissue inhibitor of metalloproteases; ACAN = aggrecan; COL = collagen; SOX9 = SRY (sex determining region Y)-Box 9; HSPG2 = heparan sulfate proteoglycan 2 (perlecan); GAPDH = glyceraldehyde-3-phosphate dehydrogenase.

COL6A1 and DCN (decorin) were indeed upregulated in female chondrocytes, while COL9A1 was upregulated in male chondrocytes (**Fig. 5F-H**). No differences were detected in HSPG2 (perlecan) expression (**Fig. 5I**).

In the context of homeostatic (non-inflammatory) matrix remodeling, the basal expression of the aggrecanases ADAMTS4 and ADAMTS5 was not dimorphic (**Fig. 5J, K**). Likewise, matrix MMPs MMP1, MMP9, and MMP13 had no differences between sexes, although MMP3 showed a trend to be higher in female cells with  $P = 0.0515$  (**Fig. 5L-O**). The expression of TIMP1 and TIMP2 was also similar between males and females (**Fig. 5P, Q**).

Taken together, these data show that male and female chondrocytes differentially express SOX9, COL6A1, COL9A1, and DCN, which can contribute to different abundances of PCM proteins in cartilage tissue.

### Dimorphism in Chondrocyte Catabolic Function

Because male and female chondrocytes showed a differential gene expression under basal conditions, we next sought

to determine whether there are sex differences in chondrocytes' catabolic function that can affect ECM remodeling. Catabolism is the hallmark of cartilage degradation and the progression of OA and can directly affect matrix mechanics. To induce catabolic function, chondrocytes were treated with 10 ng/ml of IL-1 $\beta$  for 24 hours. COL2A1 and ACAN expressions were drastically reduced after treatment, with no difference between male and female chondrocytes (**Fig. 6A, B**). SOX9 expression was reduced for both with resulting relative quantities of expression no different between sexes (**Fig. 6C**). Similar to the other ECM proteins, COL10A1 and COL11A1 were reduced for both sexes with no dimorphism (**Fig. 6D, E**). However, while the resulting relative quantity of COL6A1 and HSPG2 after treatment showed no dimorphism, the resulting expression of COL9A1 was still lower in females and DCN was still lower in males (**Fig. 6F-I**).

In terms of matrix proteases, ADAMTS4 and ADAMTS5 were upregulated in both sexes, but their increase in expression was not as much as the increase in the expression of MMPs. ADAMTS4 upregulation was higher in males (**Fig. 6J, K**). A



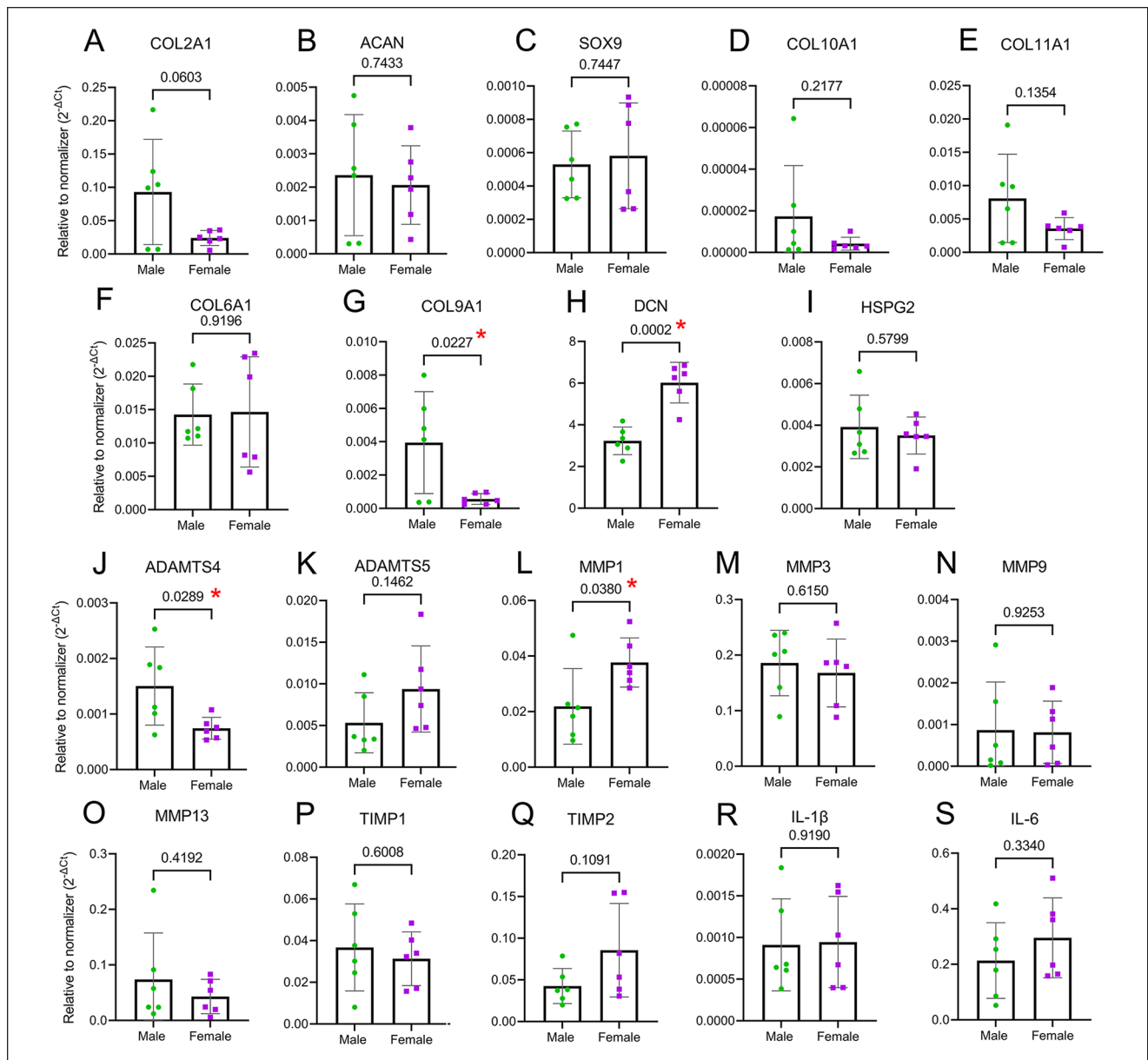


**Figure 6.** Catabolic function elicits a dimorphic response. Chondrocytes were treated with 10 ng/ml IL-1 $\beta$  for 24 hours to provoke an inflammatory response and activate the catabolic function. No differences were detected in the expression of COL2A1, ACAN, SOX9 (A-C), COL10A1, and COL11A (D-E). COL6A1 decreased similarly for males and females (F), but COL9A1 and DCN decreased, resulting in the same trend observed for basal conditions (G-H). No dimorphism was found for HSPG2 (I). All proteases tested increased with treatment (J-O), but dimorphism was observed only in ADAMTS4 and MMP1. No significant differences were detected in TIMP1 and TIMP2 expression (P-Q). The pro-inflammatory cytokines IL-1 $\beta$  and IL-6 increased with treatment; however, no dimorphism was detected (R-S). Data are presented as mean  $\pm$  SD of relative quantity to normalizer (geometric mean of 18S and GAPDH). Cells from 6 $\sigma$  + 6 $\text{f}$  were used in passage 0. MMP = metalloprotease; ADAMTS = a disintegrin and metalloproteinase with thrombospondin motifs; DCN = decorin; TIMP = tissue inhibitor of metalloproteases; ACAN = aggrecan; COL = collagen; SOX9 = SRY (sex determining region Y)-Box 9; HSPG2 = heparan sulfate proteoglycan 2 (perlecan); GAPDH = glyceraldehyde-3-phosphate dehydrogenase.

robust increase in the gene expression of MMP1, MMP3, MMP9, and MMP13 was observed for both male and female chondrocytes after IL-1 $\beta$  treatment. While no dimorphism was observed in MMP3, MMP9, and MMP13, a greater expression of MMP1 was found in females (Fig. 6L-O). However, the

expression of TIMP1 was not affected by IL-1 $\beta$ . No dimorphism was observed for TIMP1 and TIMP2 (Fig. 6P, Q). In terms of pro-inflammatory cytokines, a substantial increase in IL-6 and IL-1 $\beta$  expression occurred in both sexes. No dimorphic response was found for IL-6 or IL-1 $\beta$  (Fig. 6R, S).

Taken together, we showed that male and female chondrocytes respond differentially to a pro-inflammatory stimulation induced by IL-1 $\beta$ . ADAMTS4 upregulation was higher in males, while MMP1 upregulation was higher in females. The expression of COL9A1 and DCN conserved the dimorphism detected in basal conditions.

### No Dimorphism in Anabolic Function

Because we found an intrinsic dimorphism in gene expression between male and female chondrocytes under both basal and catabolic conditions, we next explored whether these cells have a differential response to anabolic conditions. This is a clinically relevant question, as cartilage repair therapies such as ACI rely on the anabolic function of expanded and re-implanted chondrocytes. Identifying a potential dimorphism in chondrocyte anabolic activity could help improve and tailor current interventions. To test this, we used expanded chondrocytes as a way to mimic ACI conditions. Cells were expanded in monolayers for 2 passages (P2). Cells were then transferred to a three-dimensional (3D) microenvironment provided by alginate beads and grown for up to 2 weeks in the presence of chondrogenic media supplemented with 10 ng/ml of TGF- $\beta$ 3. Gene expression of cells in monolayers was compared with cells in beads after 1 and 2 weeks of 3D culture (**Fig. 7A**). Live and dead staining confirmed the high viability of cells grown in beads for 2 weeks (**Fig. 7B**). A very similar profile of gene expression for all targets in response to TGF- $\beta$ 3 was observed in males and females with no detected sexual dimorphism in their anabolic function (**Fig. 7C-S**). Notably, by passage 2, monolayers had lost the dimorphic expression observed in basal conditions (**Fig. 7C-S**).

## Discussion

Here, we have challenged the idea that sexual dimorphism is restricted to menopause. To overcome the difficulties of obtaining young and healthy human cartilage, in this initial exploration we used bovine knee cartilage as a model. Cows have a significant reduction in fertility by 13-15 years old<sup>22,23</sup>; therefore, our model—equivalent to 18- to 20-years old in human—represents premenopausal and sexually mature age. Male cartilage had a higher abundance of network crosslinking proteins, such as fibulins and lysyl oxidase-like 2 (LOXL-2), compared with female cartilage. Moreover, male and female tissue differed in their enrichment of PCM components, and this difference is intrinsic to the chondrocyte's chromosomal sex. Indeed, we observed a dimorphic gene expression depending on the specific stimulation (**Fig. 8**). These data indicate the existence of subtle dimorphic structural differences with significant consequences for cartilage mechanics. Previous clinical evidence using MRI has revealed sex differences in cartilage at

childhood and at early adulthood.<sup>24-28</sup> Moreover, a recent report that analyzed the transcriptome of healthy knee cartilage from men and women revealed 36 sex-specific differential expression genes (DEGs), indicating sex differences at the molecular level. Although the scope of that study was not to compare pre- and postmenopausal age, the donors were young, with an age range of 27 to 57 years for females ( $n = 5$ , mean age 42 years), and 18 to 61 years for males ( $n = 13$ , mean age 34.5 years).<sup>29</sup> The combination of pre- and postmenopausal age cartilage in that investigation might be masking significant sex differences in additional genes. Indeed, our data provide additional evidence of intrinsic sex differences at the structural level of cartilage at early adulthood, highlighting the need to study cartilage at premenopausal age.

After the depletion of cells and proteoglycans to yield a collagen-enriched matrix, a 1.5-fold reduction in the moduli was observed, independent of the sex of the sample. Noticeably, the difference in moduli from male and female cartilage was still 3.45-fold, the same as for intact cartilage, suggesting that dimorphic mechanics may likely originate at the collagen network level and not due to the difference in the proteoglycan content. However, no sexual dimorphism was found in collagen type II content, indicating that other ECM components may drive the observed difference in the modulus.

Proteomic and pathway analysis of the collagen-enriched samples revealed male and female cartilage had differentially enriched pathways. Male cartilage had increased abundance of proteins associated with stabilization of recently formed collagen II fibrils and further stabilization of the matrix by crosslinking. In agreement with these results, pathways enriched in males were related to the stabilization of the ECM structure and crosslink. These findings suggest that collagen and elastin fibrils in males may have a different structural arrangement than in females. A comprehensive analysis is needed of collagen matrix structure in male and female tissue to fully decode matrix dimorphism and will follow this study. Proteins more abundant in males interconnect collagen fibrils and connect fibrils to other ECM components, strengthening network interactions. For example, collagen type IX, which was enriched in male cartilage, regulates the fibril diameter of collagen type II and connects collagen with other ECM members.<sup>30-32</sup> Nidogen-2 and fibulin-1 and -4 were also enriched in male cartilage, and both proteins participate in the repair process of elastin fibers post-damage and in elastin and collagen fibril crosslinking by allowing the proteolytic activation of LOXs.<sup>33,34</sup> Indeed, male tissue was enriched in LOXL-2. These proteins are copper-dependent amine oxidases that crosslink collagen and affect the mechanical properties of cartilage by stabilizing the network.<sup>35</sup> Collagen type XII, however, helps absorb tensile stress,<sup>36,37</sup> further favoring network stabilization in male cartilage.

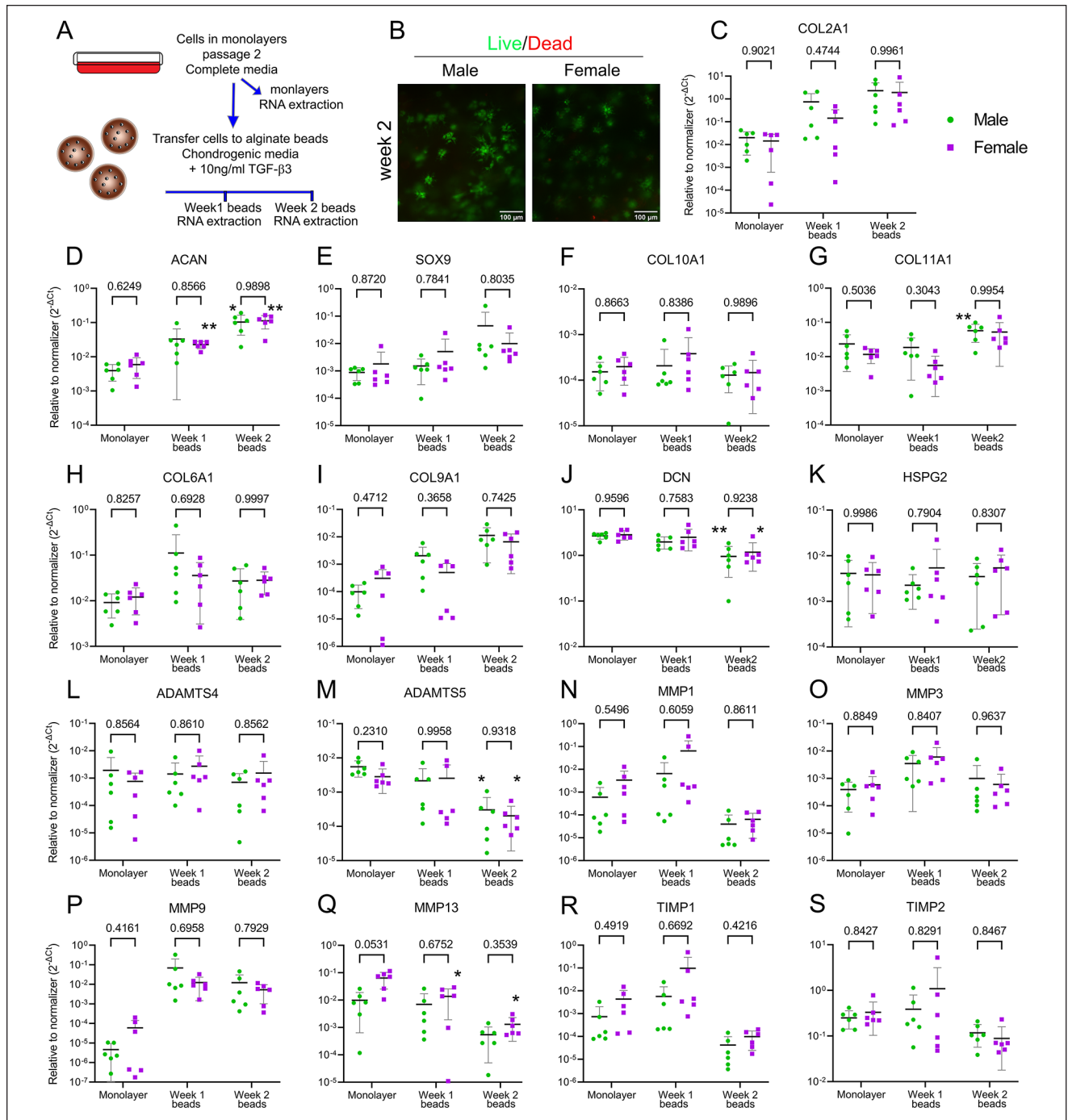


**Figure 7.** No dimorphism was detected in chondrocyte regenerative function. **(A)** Schematics of the experimental design. **(B)** Representative images showing high viability of cells kept for up to 2 weeks in alginate beads in the presence of 10 ng/ml of TGF-β3. Live cells are in green (calcein) and dead are in red (ethidium homodimer-1; scale bar, 100 μm). **(C-S)** A qPCR analysis was done on the expression of COL2A1, ACAN, SOX9, COL6A1, COL9A1, COL10A1, COL11A1, MMP1, MMP3, MMP9, MMP13, ADAMTS4, ADAMTS5, TIMP1, and TIMP2. Data are shown as mean ± SD of relative quantity to normalizer (18S and SDHA were used as normalizers). Males are shown as green circles and females as purple squares. Cells originate from 6♂ + 6♀ in passage 2. Shown P values indicate comparison between sexes per time point (two-way ANOVA with Sidak's test for multiple comparisons). The \* indicates  $P < 0.05$  and \*\* indicates  $P < 0.001$  comparing relative quantities of Week 1 to monolayer and Week 2 to monolayer per sex (repeated measures two-way ANOVA with Dunnett's test for multiple comparisons). TGF-β3 = transforming growth factor β3; qPCR = quantitative polymerase chain reaction; MMP = metalloproteinase; ADAMTS = a disintegrin and metalloproteinase with thrombospondin motifs; ACAN = aggrecan; COL = collagen; SOX9 = SRY (sex determining region Y)-Box 9; HSPG2 = heparan sulfate proteoglycan 2 (perlecan); SDHA = succinate dehydrogenase complex flavoprotein subunit A; TIMP = tissue inhibitor of metalloproteinases; ANOVA = analysis of variance.

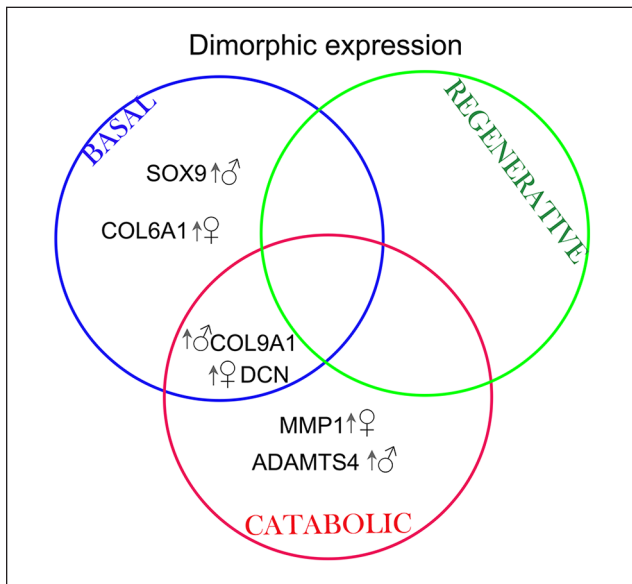


**Figure 8.** Venn diagram summarizing the targets that were differentially regulated in male and female chondrocytes depending on the particular stimulation. Arrow and symbol indicate which biological sex had an upregulated gene expression. MMP = metalloprotease; ADAMTS = a disintegrin and metalloproteinase with thrombospondin motifs; DCN = decorin; COL = collagen; SOX9 = SRY (sex determining region Y)-Box 9.

In contrast, proteins that were more abundant in female cartilage are primarily localized in the vicinities of the cell and have roles associated with cell adhesion to the PCM (vitronectin)<sup>38</sup> and PCM structural proteins. Indeed, one of the enriched pathways in females was integrin cell surface interactions and NCAM1 interactions, which involve cell binding to the ECM. The PCM forms the narrow capsule covering chondrocytes, which is crucial for mechanotransduction.<sup>39-42</sup> The specific protein composition of the PCM matrix determines its mechanical properties.<sup>43</sup> From the PCM targets that we analyzed by immunofluorescence to validate our proteomics data, we found that collagen type VI, perlecan, and decorin were mostly present in the PCM area. Collagen type IX was distributed throughout the tissue. We did not observe dimorphism in the staining pattern of perlecan, and we did not detect sex differences in the expression level of its gene, HSPG2. The fold change obtained in proteomics was enriched 1.28 times more in males compared with females. It is possible that there is a small fraction of perlecan that remains associated with the collagen matrix in our collagen-enriched protocol, and that this is more abundant in male tissue. A proteomic analysis of intact cartilage holds the answer.

In terms of decorin and collagen VI, we consistently found that these proteins were enriched in the PCM of female tissue and that their gene expression was upregulated in female chondrocytes. This indicates that

chondrocytes express differential amounts of these targets based on their chromosomal constituency. This raises the question of whether males and females have an intrinsic differential mechanotransduction mechanism or if the mechanostimulation that they receive is differential as determined by sex-based PCM and/or ECM matrix elasticity. We argue that dimorphism at the PCM could potentially impact the way chondrocytes respond to mechanical stimulation and regulate cartilage homeostasis.

The expression of SOX9 under basal conditions was upregulated in male compared with female cells. However, the expression of COL2A1 and ACAN, which are controlled by SOX9<sup>44,45</sup> was not dimorphic. However, the expression of COL9A1, also controlled by SOX9,<sup>46</sup> was upregulated in males as well. It is possible that additional mechanisms controlling COL2A1 and ACAN expression are involved.

In the regenerative function, male and female chondrocytes responded in a comparable manner; no dimorphic gene expression of the selected targets was observed. This experiment used expanded chondrocytes up to passage 2 to mimic the *in vitro* cellular expansion required for ACI, a broadly used therapy for cartilage repair. The absence of dimorphic signature suggests that under chondrogenic conditions, male and female expanded chondrocytes have a comparable potential for ECM synthesis and formation. Noticeably, cell expansion gradually decreased the observed dimorphism in gene expression (unpublished data). By passage 2, chondrocytes did not show the same dimorphism observed in cells in passage 0, indicating that the events involved in the control of sex differences might be sensitive to the mechanical environment and the chondrogenic phenotype. Further investigation of this phenomenon is ongoing in our lab.

In terms of the basal expression of catabolic markers, only MMP3 showed a trend ( $P = 0.0515$ ; **Fig. 5M**) of a higher expression in female cells. MMP3 not only regulates the function of other MMPs by cleaving their inhibitory peptide but also digests collagen type IX.<sup>47</sup> When the catabolic function was tested, we found that the expression of the aggrecanase ADAMTS4 was higher in males while the collagenase MMP1 was higher in females. Although the functional product of these proteases is further downstream gene expression (protein synthesis and activation), this raises the possibility that tissue remodeling might be different in males and females.

Our study has some limitations. It is likely that our sample preparation protocol for collagen enrichment affects matrix mechanics. However, we exposed samples simultaneously to the same protocol; therefore, we expected equivalent depletion across samples. Future studies, including those involving transcriptomics on freshly isolated cells and cells exposed to physiological oxygen conditions, are needed to further reveal dimorphic signatures for different

biological functions. Due to the high variability between samples and to the limited number of proteins in the collagen-enriched, we considered *P* values instead of adjusted *P* values. However, our mRNA expression data confirmed differential expression of COL6A1, COL9A1, and DCN, and a differential response to inflammation. We are conducting proteomic analysis of intact cartilage to unmask additional differences. The male population used in this study was not entirely representative of a human male population due to the lack of sex hormones. However, it gives an indication of cartilage regulation that is based solely on XY chromosomes in the absence of sex hormones. Our initial exploration in bovine samples provides insights into sexual dimorphism in the musculoskeletal system; however, further investigation is needed to reveal a similar trend in human cartilage.

Understanding sexual dimorphism in articular cartilage mechanics and homeostasis determined by chromosomal sex can have significant consequences for the management of musculoskeletal diseases and for cartilage-regenerative medicine. Current clinical interventions, such as osteochondral implants or ACI, rely on ECM synthesis and the regulation of the catabolic response. Cartilage repair using these approaches could be tailored to target sex-specific responses.

### Authors Contributions

Conceptualization: P.H. and Y.D. Data acquisition: Z.B., C.H., M.M., J.W., and P.H. Data analysis: P.H., C.H., Z.B., M.M., A.S., C.X., J.W., and T.W. Supervision: P.H. Data interpretation: P.H., C.H., C.X., A.S., Y.D., Z.B., and M.M. All authors contributed to writing and approving the manuscript for publication. All data obtained in this study are shown in results and in supplementary information. Proteomics data will be uploaded to a public repository upon publication of this manuscript.

### Acknowledgments and Funding

The authors thank the Proteomics Core, the Histopathology Core, and the Quantitative Light Microscopy Core (1S10OD021684-01 to Kate Luby-Phelps) at UT Southwestern Medical Center. The authors also thank Dr. Jonathan Rios, Dr. Carol Wise, and Dr. John Wardale for their comments on the manuscript, as well as Dave Primm for help in editing it. The author(s) disclosed receipt of the following financial support for the research, authorship, and/or publication of this article: Funding was provided by the Department of Orthopaedic Surgery at UT Southwestern Medical Center.

### Declaration of Conflicting Interests


The author(s) declared no potential conflicts of interest with respect to the research, authorship, and/or publication of this article.

### Ethical Approval

No IRB or IACUC was required for this study.

### ORCID iDs

Paula A. Hernandez  <https://orcid.org/0000-0002-8785-7351>

Miranda Moreno  <https://orcid.org/0000-0002-4577-8380>

Chao Xing  <https://orcid.org/0000-0002-1838-0502>

Tre Welch  <https://orcid.org/0000-0003-3645-3442>

### References

- Hewett TE, Myer GD, Ford KR. Anterior cruciate ligament injuries in female athletes: Part 1, mechanisms and risk factors. *Am J Sports Med.* 2006;34(2):299-311. doi:10.1177/0363546505284183.
- Hosseinzadeh S, Kiapour AM. Sex differences in anatomic features linked to anterior cruciate ligament injuries during skeletal growth and maturation. *Am J Sports Med.* 2020;48(9):2205-12. doi:10.1177/0363546520931831.
- Racine J, Aaron RK. Post-traumatic osteoarthritis after ACL injury. *R I Med J.* 2014;97(11):25-8.
- Boyan BD, Tosi L, Coutts R, Enoka R, Hart DA, Nicoletta DP, *et al.* Sex differences in osteoarthritis of the knee. *J Am Acad Orthop Surg.* 2012;20(10):668-9. doi:10.5435/jaaos-20-10-668.
- Hame SL, Alexander RA. Knee osteoarthritis in women. *Curr Rev Musculoskelet Med.* 2013;6(2):182-7. doi:10.1007/s12178-013-9164-0.
- Payne KA, Didiano DM, Chu CR. Donor sex and age influence the chondrogenic potential of human femoral bone marrow stem cells. *Osteoarthritis Cartilage.* 2010;18(5):705-13. doi:10.1016/j.joca.2010.01.011.
- Li Y, Wen Y, Green M, Cabral EK, Wani P, Zhang F, *et al.* Cell sex affects extracellular matrix protein expression and proliferation of smooth muscle progenitor cells derived from human pluripotent stem cells. *Stem Cell Res Ther.* 2017;8(1):156. doi:10.1186/s13287-017-0606-2.
- Nasatzky E, Schwartz Z, Boyan BD, Soskolne WA, Ornoy A. Sex-dependent effects of 17-beta-estradiol on chondrocyte differentiation in culture. *J Cell Physiol.* 1993;154(2):359-67. doi:10.1002/jcp.1041540220.
- Kinney RC, Schwartz Z, Week K, Lotz MK, Boyan BD. Human articular chondrocytes exhibit sexual dimorphism in their responses to 17-beta-estradiol. *Osteoarthritis Cartilage.* 2005;13(4):330-7. doi:10.1016/j.joca.2004.12.003.
- Schwartz Z, Nasatzky E, Ornoy A, Brooks BP, Soskolne WA, Boyan BD. Gender-specific, maturation-dependent effects of testosterone on chondrocytes in culture. *Endocrinology.* 1994;134(4):1640-7. doi:10.1210/endo.134.4.8137726.
- Kreuz PC, Müller S, von Keudell A, Tischer T, Kaps C, Niemeyer P, *et al.* Influence of sex on the outcome of autologous chondrocyte implantation in chondral defects of the knee. *Am J Sports Med.* 2013;41(7):1541-8. doi:10.1177/0363546513489262.
- Gokulakrishnan P, Kumar RR, Sharma BD, Mendiratta SK, Sharma D. Sex determination of cattle meat by polymerase chain reaction amplification of the DEAD box protein (DDX3X/DDX3Y) Gene. *Asian-Australas J Anim Sci.* 2012;25(5):733-7. doi:10.5713/ajas.2012.12003.
- Alibegovic A, Blagus R, Martinez IZ. Safranin O without fast green is the best staining method for testing the degradation of macromolecules in a cartilage extracellular matrix for the

- determination of the postmortem interval. *Forensic Sci Med Pathol.* 2020;16(2):252-8. doi:10.1007/s12024-019-00208-0.
14. Bautista CA, Bilgen B. Decellularization and recellularization of cartilage. *Methods Mol Biol.* 2018;1577:139-46. doi:10.1007/7651\_2017\_59.
  15. Hernandez PA, Jacobsen TD, Barati Z, Chahine NO. Confocal scanning of intervertebral disc cells in 3D: inside alginate beads and in native microenvironment. *JOR Spine.* 2020;3(4):e1106. doi:10.1002/jsp2.1106.
  16. Johnson ECB, Dammer EB, Duong DM, Ping L, Zhou M, Yin L, *et al.* Large-scale proteomic analysis of Alzheimer's disease brain and cerebrospinal fluid reveals early changes in energy metabolism associated with microglia and astrocyte activation. *Nat Med.* 2020;26(5):769-80. doi:10.1038/s41591-020-0815-6.
  17. Benjamini Y, Hochberg Y. Controlling the false discovery rate: a practical and powerful approach to multiple testing. *J R Stat Soc Series B Stat Methodol.* 1995;57(1):289-300.
  18. Armstrong CG, Mow VC. Variations in the intrinsic mechanical properties of human articular cartilage with age, degeneration, and water content. *J Bone Joint Surg Am.* 1982;64(1):88-94.
  19. Inerot S, Heinegard D, Audell L, Olsson SE. Articular cartilage proteoglycans in aging and osteoarthritis. *Biochem J.* 1978;169(1):143-56. doi:10.1042/bj1690143.
  20. Bautista CA, Park HJ, Mazur CM, Aaron RK, Bilgen B. Effects of chondroitinase ABC-mediated proteoglycan digestion on decellularization and recellularization of articular cartilage. *PLoS ONE.* 2016;11(7):e0158976. doi:10.1371/journal.pone.0158976.
  21. Liao Y, Wang J, Jaehnig EJ, Shi Z, Zhang B. WebGestalt 2019: gene set analysis toolkit with revamped UIs and APIs. *Nucleic Acids Res.* 2019;47(W1):W199-W205. doi:10.1093/nar/gkz401.
  22. Malhi PS, Adams GP, Singh J. Bovine model for the study of reproductive aging in women: follicular, luteal, and endocrine characteristics. *Biol Reprod.* 2005;73(1):45-53. doi:10.1095/biolreprod.104.038745.
  23. Erickson BH, Reynolds RA, Murphree RL. Ovarian characteristics and reproductive performance of the aged cow. *Biol Reprod.* 1976;15(4):555-60. doi:10.1095/biolreprod15.4.555.
  24. Jousse-Joulin S, Cangemi C, Alavi Z, Gerard S, Nonent M, Bressollette L, *et al.* Normal sonoanatomy of small joints in healthy children: changes in cartilage and vascularisation according to age and gender. *Clin Exp Rheumatol.* 2018;36(6):1103-9.
  25. Jones G, Ding C, Glisson M, Hynes K, Ma D, Cicuttini F. Knee articular cartilage development in children: a longitudinal study of the effect of sex, growth, body composition, and physical activity. *Pediatr Res.* 2003;54(2):230-6. doi:10.1203/01.PDR.0000072781.93856.E6.
  26. Kim HK, Shiraj S, Anton CG, Horn PS, Dardzinski BJ. Age and sex dependency of cartilage T2 relaxation time mapping in MRI of children and adolescents. *AJR Am J Roentgenol.* 2014;202(3):626-32. doi:10.2214/AJR.13.11327.
  27. Bedewi MA, Elsifey AA, Naguib MF, Saleh AK, Nwihadh NB, Abd-Elghany AA, *et al.* Sonographic assessment of femoral cartilage thickness in healthy adults. *J Int Med Res.* 2020;48(8):300060520948754. doi:10.1177/0300060520948754.
  28. Ding C, Cicuttini F, Scott F, Glisson M, Jones G. Sex differences in knee cartilage volume in adults: role of body and bone size, age and physical activity. *Rheumatology.* 2003;42(11):1317-23. doi:10.1093/rheumatology/keg374.
  29. Li C, Zheng Z. Males and females have distinct molecular events in the articular cartilage during knee osteoarthritis. *Int J Mol Sci.* 2021;22(15):7876. doi:10.3390/ijms22157876.
  30. Chen CH, Yeh ML, Geyer M, Wang GJ, Huang MH, Heggenes MH, *et al.* Interactions between collagen IX and biglycan measured by atomic force microscopy. *Biochem Biophys Res Commun.* 2006;339(1):204-8. doi:10.1016/j.bbrc.2005.10.205.
  31. Eyre DR, Pietka T, Weis MA, Wu JJ. Covalent cross-linking of the NC1 domain of collagen type IX to collagen type II in cartilage. *J Biol Chem.* 2004;279(4):2568-74. doi:10.1074/jbc.M311653200.
  32. Diab M, Wu JJ, Eyre DR. Collagen type IX from human cartilage: a structural profile of intermolecular cross-linking sites. *Biochem J.* 1996;314(Pt 1):327-32. doi:10.1042/bj3140327.
  33. Roark EF, Keene DR, Haudenschild CC, Godyna S, Little CD, Argraves WS. The association of human fibulin-1 with elastic fibers: an immunohistological, ultrastructural, and RNA study. *J Histochem Cytochem.* 1995;43(4):401-11. doi:10.1177/43.4.7534784.
  34. Horiguchi M, Inoue T, Ohbayashi T, Hirai M, Noda K, Marmorstein LY, *et al.* Fibulin-4 conducts proper elastogenesis via interaction with cross-linking enzyme lysyl oxidase. *Proc Natl Acad Sci U S A.* 2009;106(45):19029-34. doi:10.1073/pnas.0908268106.
  35. Depalle B, Qin Z, Shefelbine SJ, Buehler MJ. Influence of cross-link structure, density and mechanical properties in the mesoscale deformation mechanisms of collagen fibrils. *J Mech Behav Biomed Mater.* 2015;52:1-13. doi:10.1016/j.jmbbm.2014.07.008.
  36. Fluck M, Giraud MN, Tunc V, Chiquet M. Tensile stress-dependent collagen XII and fibronectin production by fibroblasts requires separate pathways. *Biochim Biophys Acta.* 2003;1593(2-3):239-48. doi:10.1016/s0167-4889(02)00394-4.
  37. Chiquet M, Birk DE, Bonnemant CG, Koch M. Collagen XII: protecting bone and muscle integrity by organizing collagen fibrils. *Int J Biochem Cell Biol.* 2014;53:51-4. doi:10.1016/j.biocel.2014.04.020.
  38. Freed E, Gailit J, van der Geer P, Ruoslahti E, Hunter T. A novel integrin beta subunit is associated with the vitronectin receptor alpha subunit (alpha v) in a human osteosarcoma cell line and is a substrate for protein kinase C. *EMBO J.* 1989;8(10):2955-65. doi:10.1002/j.1460-2075.1989.tb08445.x.
  39. Chery DR, Han B, Zhou Y, Wang C, Adams SM, Chandrasekaran P, *et al.* Decorin regulates cartilage pericellular matrix micromechanobiology. *Matrix Biol.* 2021;96:1-17. doi:10.1016/j.matbio.2020.11.002.
  40. Guilak F, Hayes AJ, Melrose J. Perlecan in pericellular mechanosensory cell-matrix communication, extracellular matrix stabilisation and mechanoregulation of load-bearing

- connective tissues. *Int J Mol Sci.* 2021;22(5):2716. doi:10.3390/ijms22052716.
41. Zelenski NA, Leddy HA, Sanchez-Adams J, Zhang J, Bonaldo P, Liedtke W, *et al.* Type VI collagen regulates pericellular matrix properties, chondrocyte swelling, and mechanotransduction in mouse articular cartilage. *Arthritis Rheumatol.* 2015;67(5):1286-94. doi:10.1002/art.39034.
  42. Guilak F, Alexopoulos LG, Upton ML, Youn I, Choi JB, Cao L, *et al.* The pericellular matrix as a transducer of biomechanical and biochemical signals in articular cartilage. *Ann N Y Acad Sci.* 2006;1068:498-512. doi:10.1196/annals.1346.011.
  43. Wilusz RE, Defrate LE, Guilak F. A biomechanical role for perlecan in the pericellular matrix of articular cartilage. *Matrix Biol.* 2012;31(6):320-7. doi:10.1016/j.matbio.2012.05.002.
  44. Bell DM, Leung KK, Wheatley SC, Ng LJ, Zhou S, Ling KW, *et al.* SOX9 directly regulates the type-II collagen gene. *Nat Genet.* 1997;16(2):174-8. doi:10.1038/ng0697-174.
  45. Sekiya I, Tsuji K, Koopman P, Watanabe H, Yamada Y, Shinomiya K, *et al.* SOX9 enhances aggrecan gene promoter/enhancer activity and is up-regulated by retinoic acid in a cartilage-derived cell line, TC6. *J Biol Chem.* 2000;275(15):10738-44. doi:10.1074/jbc.275.15.10738.
  46. Genzer MA, Bridgewater LC. A Col9a1 enhancer element activated by two interdependent SOX9 dimers. *Nucleic Acids Res.* 2007;35(4):1178-86. doi:10.1093/nar/gkm014.
  47. Okada Y, Konomi H, Yada T, Kimata K, Nagase H. Degradation of type IX collagen by matrix metalloproteinase 3 (stromelysin) from human rheumatoid synovial cells. *FEBS Lett.* 1989;244(2):473-6. doi:10.1016/0014-5793(89)80586-1.